Microgrid for Remote Areas with Water Pumping, based on Wind-Diesel DER and Energy Storage

Marcelo G. Cendoya[2], Graciela M. Toccaceli[2], Pedro E. Battaiotto, Roberto J. Vignoni[2]
Instituto LEICI, Facultad de Ingeniería, Universidad Nacional de La Plata (UNLP),
La Plata, Buenos Aires, Argentina
cendoya@ing.unlp.edu.ar, toccaceli@ing.unlp.edu.ar, pedro@ing.unlp.edu.ar, vignoni@ing.unlp.edu.ar

***Abstract*— In remote regions were a main distribution grid is not available, the implementation of Microgrids with Distributed Energy Resources (DERs) are very useful. In this context, a Stand-Alone Wind/Diesel Microgrid with modular architecture is proposed. The main scope is to feed Residential loads and a Water Pumping System through a local AC BUS. The random characteristics of the wind makes necessary to smooth the fluctuating supply in order to minimize disturbances in the pump and diesel generator. To overcome this problem, a compensation control strategy based in the power control of a Storage Energy System and the Water Pumping System is employed. An appropriate and reliable communication network is used to supervise and balance generation and loads, to maintain the correct functioning of the Microgrid. The system structure, operation and mathematical models for simulation and validation are presented.**

***Index Terms*-- flywheel, microgrid, pumping, wind/diesel generators, distributed energy resources.**

I. INTRODUCTION

In remote areas, far from the electric power grid, the autonomous generation based on the Microgrid concept with Distributed Energy Resources (DERs) [1][2] constitutes a very useful alternative to provide electric energy. This generation and distribution, since most devices will be normalized and commercially available, it is convenient to be of AC with fixed frequency and voltage of standard values [8][9]. In this isolated regions, among others, loads of particular importance are Pumping Systems (PS) and Residential Consumption (RC). This work proposes and analyzes a modular structure with distributed generation and energy storage. It is based on a variable speed Wind Generator (WG), a Diesel/Gas Generator (D/GG) and a Flywheel (FW) storage system to minimize fast wind fluctuations [3][4].

The system modules are connected through a local AC power grid. The D/GG provides fixed voltage and frequency and the minimum base power needed for the PS and RC. This assures a minimum electrical service in absence of wind. An electronic PLC based Supervisor Control System take actions depending on the mechanical and electrical variables of each module. An adequate control strategy applied to the FW allows smoothing the power fluctuations due to fast variations on wind speed. This permits to attenuate perturbations on the D/GG and PS systems, reducing mechanical fatigue. The control strategy applied on the PS improves pump performance and reduces D/GG fuel/gas consumption.

This work presents preliminary results, considering different aspects related to the system configuration, conversion strategy, energy control and the mathematical models used for simulation.

II. SYSTEM STRUCTURE

The system configuration is shown in Fig. 1.The D/GG is a three-phase synchronous machine driven by a diesel engine or a gas turbine, which feeds directly a residential AC load. The generator has associated the usual control systems, maintaining a regulated voltage and frequency. A transformer adapts the D/GG AC output voltage to the input voltage required by the Matrix Converters (MC) that feed the Induction Machines (IM) of the system, because such converters are of step-down type. The WG is integrated by a three blade HAWT with fixed pitch, which makes the eolic–mechanic conversion at variable speed and drives through a gearbox a 3-phase Induction Generator (IG) for the mechanical–electrical conversion. A closed loop controls the antagonist torque that the IG opposes to the turbine following an external reference T_g*. This allows the IG to hand over the optimal speed for each wind speed at steady state. The control loop acts over the IG frequency and feeding voltage, keeping V/f constant. The IG works with speeds lower or equal than the rated values. The PS is formed by a centrifugal pump driven by a three-phase IM. A closed loop controls the consumed power from the D/GG, modifying the pump speed following an external reference P_{link}*. This loop actuates over the IM frequency and voltage, in order to keep constant flux (V/f= cte). The FW module has a wheel with high moment of inertia driven by a three-phase IM. A close loop controls the driving torque following an external reference T_{fw}*, which allows

[2] Consejo Nacional de Investigaciones Científicas y Técnicas (CONICET)

978-1-4673-6605-2/15/$31.00 ©2015 IEEE

to vary the flywheel speed and hence its stored energy. The loop acts varying the feeding frequency above the rated value while keeping the rated voltage, making the IM to operate in the field weakening region. Then, more energy storage capacity is obtained working at higher speeds. Due to the high FW inertia, a drive with fast dynamic response is not required. The supervisor control module operates the whole system, imposing the reference values for each module [6][7]. The supervisory task is performed considering the electrical and mechanical values measured in the system.

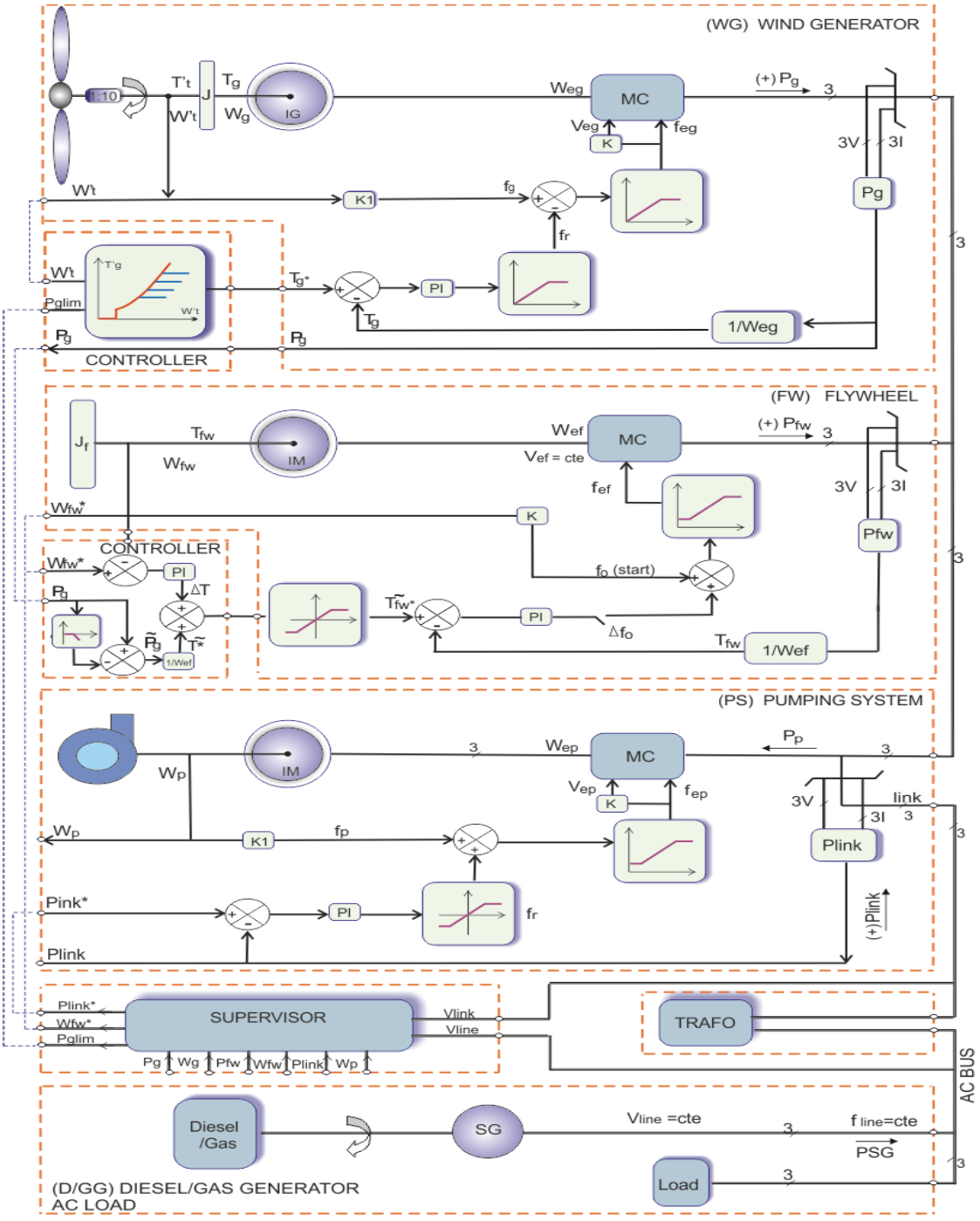

Fig. 1. Microgrid structure.

Except for the D/GG module, the rest are based in three-phase cage rotor IM, with scalar drivers of variable frequency, so the machines can work in a wide range of speeds, finding an adequate operating point for each module. The IM was chosen due to its robustness, reliability, low cost and reduced maintenance. The variable frequency voltage that feeds them is obtained through a MC which has the advantage of not having a DC-link and do not require expensive storage capacitors. The MC permits bidirectional power flow, allowing the IM to operate as motors or generators.

For the communication network between Supervisor and the other Modules, different type of protocols and/or physical media may be used [10]. In the last few years even if a lot of work has been done, still there is not an accepted standard to cover all different types of Microgrids. This is due to the high dependency between the type of communication network and different Microgrid characteristics, such us connection or non-connection to a main distribution system, geographical deployment, electromagnetic pollution, type of generation and loads, time constrains for real time messages, etc. and last but not least cost. In the proposed topology, we consider a fast Ethernet or higher (IEEE 802.3) optical fiber network. When distances makes the wired network less cost effective, a wireless ZigBee network (IEEE 802.15.4) it's being considered.

III. System Control and Operation

A. Diesel/Gas Generator

The D/GG is in charge of: 1) Set the frequency and voltage of the local AC bus, 2) Feed the Residential AC loads and maintain a base active power to guarantee a minimum pumping capacity and 3) Supply the reactive power for the whole system.

A control loop that acts over the field keeps constant the output voltage. Another control loop, acting over the engine fuel feeding, maintains a constant rotational speed and hence the frequency. The reference values of such control loops, are determined by the requirements of the AC load.

B. Wind Generator

The power developed by a wind turbine P_t is:

$$P_t = C_P(\lambda) P_w = C_P(\lambda) 0.5 \rho A v^3 \quad (1)$$

where: $C_p(\lambda)$: power coefficient; $\lambda = r\omega / v$: tip speed ratio; ω_t: turbine speed ; P_w: wind power; ρ: air density; $A = \pi r^2$: capture area; r: blade radius ; v: wind speed.

The torque produced by the turbine T_t will be:

$$P_t = T_t \omega_t \Rightarrow T_t = C_P(\lambda) 0.5 \rho A r v^2 / \lambda \quad (2)$$

represented in Fig. 2 for different values of wind speed. P_{tmax} is obtained with $C_{Pmax} = C_P(\lambda_o)$, been λ_o the optimum tip speed.

In the T-ω plane, the corresponding P_{tmax} points describe a parabola (Fig. 2), which is given by:

$$T_{topt}(\omega_t) = k_t \omega_t^2 \quad (3)$$

with $k_t = 0.5 \rho A r^3 C_{P\max} / \lambda_o^3$

From Fig.1 it can be seen that if the friction is neglected, the WG operation point in stationary state (ω=cte.) is defined by:

$$T_t' = T_g \quad (4)$$

being: T'_t: turbine torque referred to generator shaft; T_g: generator torque.

Hence, to work in a desired point, T_g must be imposed, which is obtained through a torque control loop that acts over the generator frequency and voltage. The torque is measured indirectly, sensing electric variables. In IM, if the stator loses are considered negligible, then:

$$P_s = P_{gap} = T_g \omega_{eg} \Rightarrow T_g = P_S / \omega_{eg} \quad (5)$$

with: $P_s = v_a i_a + v_b i_b + v_c i_c$: stator power; P_{gap}: air gap power; v_a, v_b *y* v_c: stator voltages; i_a ,i_b *e* i_c: stator currents; $\omega_{eg} = 2\pi f/p$: synchronous speed; f: stator frequency; p: pole pairs.

The reference torque T_g^* is determined from ω'_t y $P_{g\ limit}$, (IG power limit), as:

$$T_g^* = \begin{cases} K_T \omega_t'^2 & , \quad \omega_t' \le \omega_{cruce} \\ P_{g\ limit} / (\omega_t') & , \quad \omega_t' > \omega_{cruce} \end{cases} \quad (6)$$

with: $\omega_{cruce} = \sqrt[3]{P_{g\ limit} / K_T}$

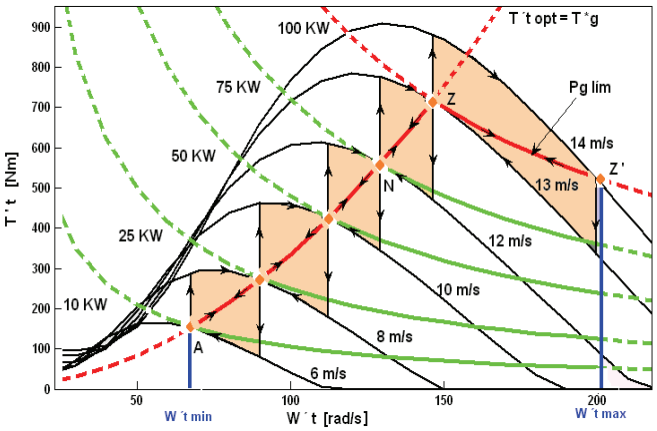

Fig. 2: WG operating points.

The locus of the IG operation points is formed by the conjunction of the T'_{topt} parabola and P_{glimit} hyperbole, depending on the ω'_t, (Fig. 2). In the same figure an evolution of the turbine and IG working points (T'_t y T_g) against wind steps in the range of 6m/s a 14m/s, is presented. After the transient, associated with the energy storage in the rotating mass of the turbine (orange area), the work points coincide with the parabola T'_{topt}, (eg. points A, N, Z). When the wind speed exceeds 13m/s, the operation points belong to the hyperbole that corresponds to P_{glimit} equal 100KW in this case. For 14m/s, the work point would be Z´. The value of ω'_t is comprised in a range limited by the minimum generation corresponding speed and the maximum speed allowed by the turbine, over which the mechanical integrity would be compromised.

C. Pumping System

It is desired the power supplied to the pump comes mainly from the WG (P_g). A control loop regulates the power from the D/GG, P_{link} to a base value set by the used reference P_{link}^*. This loop varies the pump speed ω_p, acting on the frequency and voltage of the induction motor, to change its power:

$$P_p = k_p \omega_p^3 \tag{7}$$

where k_p: constant that depends on the pump construction. For each value of P_g, the control loop will set P_p to:

$$P_p = P_g + P_{link}^* \tag{8}$$

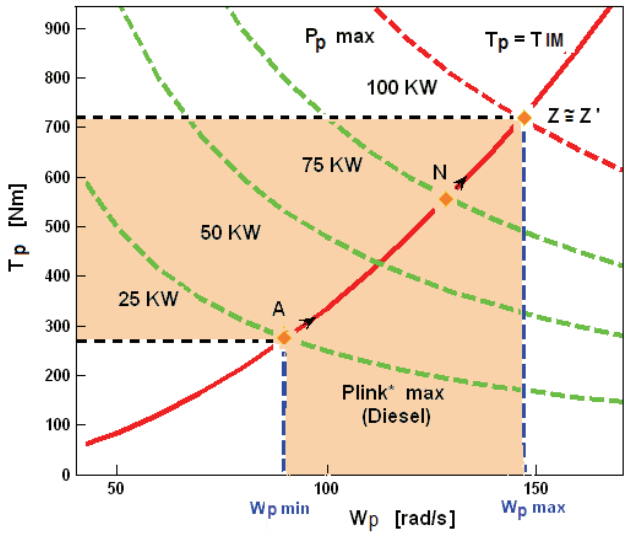

Fig. 3: PS stationary working points.

Fig. 3 shows the work points of the pump in stationary state. In A, the WG supplies 10KW and the pump absorbs 25KW for P_{link}^*=15KW (value set by the supervisory control). If P_g rises, point A will move to de right keeping P_{Link} constant. If the supervisory control would set P_{link}^*=0, then, the WG will contribute with the total P_p, shown in point N for 75KW. In Z, P_p has reached its possible maximum and the WG is limited to this same value, 100KW (see Z to Z´ in Fig.2).

D. Flywheel

Due to the random nature of the wind, the power supplied by the WG is fluctuating. Two power fluctuations can be distinguished: slow variations due to changes in the average wind speed, and fast variations caused by wind gusts. The later could be harmful for the PS operation, provoking mechanical fatigue that shortens its lifespan and worsens its performance. The FW module is used to attenuate the fast power fluctuations at the input of the PS module [5]. A control strategy with quick response is proposed, which allows storing energy when P_g is increasing and supplying energy when P_g is decreasing. If the control loop works correctly, the power handled by the FW P_{fw}, is:

$$P_{fw} = \tilde{P}_g = P_g - \overline{P}_g \tag{9}$$

where: P_g: IG total power; $\tilde{P}_g$: fast variation of P_g; $\overline{P}_g$: average value of P_g. The kinetic energy E stored by the FW is given by:

$$E = 0.5 J_{fw} \omega_{fw}^2 \tag{10}$$

with: J_{fw}: FW inertia; ω_{fw}: FW speed. For its correct operation, the FW speed must be within a certain range (ω_{fwmin}, ω_{fwmax}). Speeds above ω_{fwmax} are not allowed to limit mechanical stresses. Working at speeds below ω_{fwmi} it is useless because the stored energy is very small. Then, the useful energy variation of the FW will be:

$$\Delta E_{util} = E_{\max} - E_{\min} = E_{\max}(1 - 1/k_\omega^2) \tag{11}$$

In Ec. (11), E_{min} y E_{max} are the minimum and maximum stored energies for ω_{fwmin} and ω_{fwmax} respectively, while $k_\omega = \omega_{fwmax}/\omega_{fwmin}$ is known as speed ratio. Usually k_ω is set on 2 or 3 giving a ΔE_{util}=0,75 or 0,89E_{max}. To smooth P_g, the FW must be capable of store and supply energy anytime. It is then necessary, that in idle condition the FW operates at an intermediate speed given by:

$$E_n = (E_{\min} + E_{\max})/2 \rightarrow \omega_{fw}^* = \sqrt{\left(\omega_{fw\min}^2 + \omega_{fw\max}^2\right)/2} \tag{12}$$

In order to obtain this, a correction of the reference torque (ΔT) is introduced in the power control loop of the FW, which is obtained from a speed reference ω_{fw}^*, as indicated in Fig. 1. Hence, there is a slow control loop that regulates the average FW speed, without interfering with the smoothing action. Finally, from the above considerations, the reference torque (T_{fw}^*) for the FW loop is composed by:

$$T_{fw}^{*} = \tilde{P}_g / \omega_{efw} + \Delta T = \tilde{T}_{fW} + \Delta T \qquad (13)$$

where $\tilde{T}_{fW}$ is the reference torque of the power smoothing loop (fast) and ΔT is the torque correction introduced by the speed regulation loop (slow). As seen in Fig. 1, $\tilde{T}_{fW}$ is obtained from $\tilde{P}_g$, which is calculated in Ec. (9). This requires the knowledge of $\overline{P}_g$, which is a slow variation, and is obtained with a low pass filter.

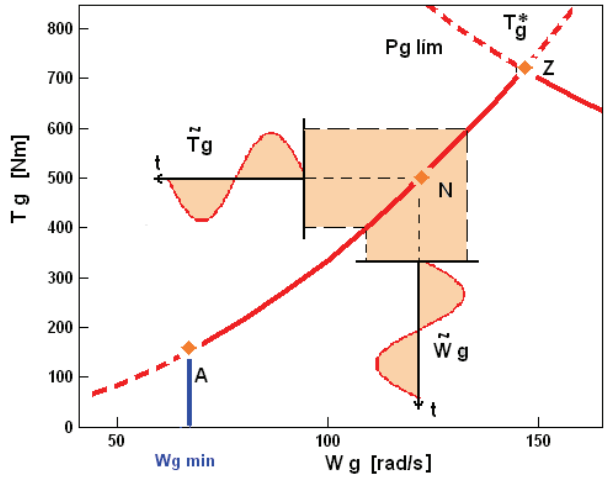

Fig. 4: WG power fluctuation.

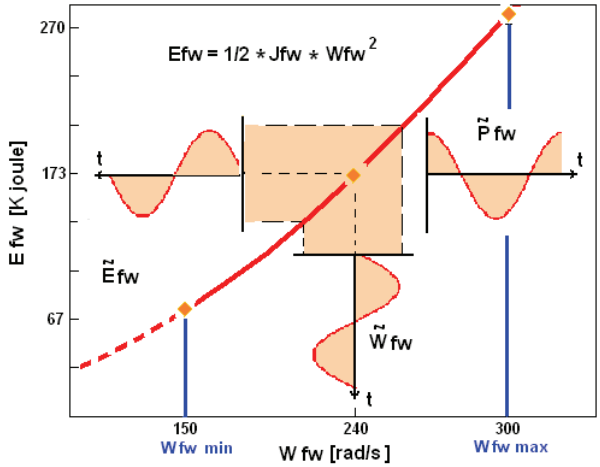

Fig. 5: FW energy fluctuation.

To illustrate the smoothing action of the FW, Fig. 4 shows an electric power fluctuation injected by the WG due to wind speed variations. This variation is considered sinusoidal for simplicity. Fig. 5 shows the storage energy fluctuations in the FW ($\tilde{E}_{fW}$) due to $\tilde{P}_g$.

E. *Supervisory Control System*

The supervisory module receives information from two sources: a) Operator/User: Maximum base power for P_p taken from the D/GG; rated values and limits for torque, speed and power for each module. b) Measurement instruments for mechanic and electric variables: P_g, ω_g, ω_{fw}, ω_p, and P_{link}.

From these values, the supervisory module will drive the WG, the FW and PS modules, fixing the reference values for the torque and power internal loops (P_{glimit}, P_{link}^{*}, ω_{fw}^{*}).

IV. System Modelling

Due to the whole system complexity and in the need to obtain results in reasonable simulation times, some of the modules are represented through simplified functional macro models.

A. *Diesel/Gas Generator - Load*

Ideal voltage and frequency control loops are supposed:

$$V_{CA} = V_{CA}^{*} \quad , \quad f = f^{*} \qquad (14)$$

The SG is modeled by means of a three-phase, symmetric ideal generator of sinusoidal voltage:

$$v_{a,b,c} = \sqrt{2} V_{CA} sen(\omega t - \theta_{a,b,c}) \qquad (15)$$

being $\omega = 2\pi f^{*}$. The AC load is represented by concentrated impedances whose values vary with the consumed active P and reactive Q powers:

$$Z_{a,b,c} = R + jX = V_{CA}^{2} P / \left(P^{2} + Q^{2}\right) + jV_{CA}^{2} Q / \left(P^{2} + Q^{2}\right) \qquad (16)$$

B. *Wind Generator*

1) *Mechanical System.*

$$T_t^{'} - T_g = J_{tg} d\omega_g / dt + B_{tg} \omega_g \ldots\ldots\ldots\ldots (17)$$

where: J_{tg}: WT+IG inertia; B_{tg}: WT+IG friction coefficient; T'_T calculated through Ec. (2) with $C_P(\lambda)$ in table or curve fitting and affected by gearbox ratio; $T_g = T_g^{*}$ calculated with Ec. (6).

2) *Generator - Driver.*

Harmonics and reactive components of the currents injected to the grid by the MC are not considered. The active components of such currents are modeled with a three-phase ideal current generator, with the following values:

$$i_{a,b,c} = \left[2\eta_g \eta_{MC} T_g \omega_g / 3\hat{V}_{CA} \right] sen(\omega t - \theta_{a,b,c}) \qquad (18)$$

where: η_g: IG efficiency; η_{MC}: MC efficiency; $\hat{V}_{CA}$: AC bus peak voltage; $\omega=2\pi f$, f: AC bus frequency; $\theta_a=0$, $\theta_b=2\pi/3$, $\theta_c=4\pi/3$.

C. Pumping System

If the close loop that controls P_{link} works correctly, P_p can be calculated through Ec. (8). The fundamental components of the currents fed to the MC will be:

$$i_{a,b,c} = \left[2P_p / 3\hat{V}_{CA}\eta_{MI}\eta_{MC} \right] sen(\omega t - \theta_{a,b,c}) \qquad (19)$$

where: η_{MI}: IM efficiency.

D. Flywheel

For this module, a more detailed model was used.

1) Mechanical System.

$$T_{MI} = T_{fw} = J_{fw} d\omega_{fw} / dt + B_{fw}\omega_{fw} \qquad (20)$$

where: T_{MI}: IM torque ; J_{fw}: FW+IM inertia; B_{fw}: FW+IM friction coefficient.

2) Induction Motor.

A classical dq dynamic model is used. The electrical equations are:

$$\begin{cases} V_{ds} = R_s i_{ds} + d\varphi_{ds}/dt - \omega\varphi_{qs} \\ V_{qs} = R_s i_{qs} + d\varphi_{qs}/dt + \omega\varphi_{ds} \\ V_{dr} = R_r i_{dr} + d\varphi_{dr}/dt - (\omega - \omega_r)\varphi_{qr} \\ V_{qr} = R_r i_{qr} + d\varphi_{qr}/dt + (\omega - \omega_r)\varphi_{dr} \end{cases} \qquad (21)$$

where: R_s, R_r: phase, stator and rotor resistances; $\omega=p\omega_{mec}$. The stator and rotor fluxes may be expressed as:

$$\begin{cases} \varphi_{ds} = L_s i_{ds} + L_m i_{dr} \\ \varphi_{qs} = L_s i_{qs} + L_m i_{qr} \\ \varphi_{dr} = L_r i_{dr} + L_m i_{ds} \\ \varphi_{qr} = L_r i_{qr} + L_m i_{qs} \end{cases} \qquad (22)$$

where: $L_s = L_{ls} + L_m$; $L_r = L_{lr} + L_m$ and i_{ds}, i_{qs}, i_{dr} e i_{qr} are the stator and rotor direct and quadrature current components, respectively. The electromagnetic torque is:

$$T_{MI} = 1.5p(\varphi_{ds} i_{qs} - \varphi_{qs} i_{ds}) \qquad (23)$$

V. Conclusions

- The modularity of the proposed system makes it highly flexible and reconfigurable both in its topology and its control.
- The constitutive parts are available in the local market and present a low maintenance costs.
- The simulation results in steady state had validated the correct functioning of internal control loops and also the system as a whole.
- The proposed control and compensation strategy results effective, significantly reducing the disturbances created by the wind random nature in the control loops of the D/GG and PS.
- The obtained results for stationary conditions, encouraging us to continue working. We are planning a second stage oriented to the study of the system dynamic behavior.

Acknowledgment

The authors wish to thank the Argentine institutions CONICET, UNLP and ANPCyT, for their support.

References

[1] J.K. Kaldellis, "Stand-alone and Hybrid Wind Energy Systems: Technology, Energy Storage and Applications", Cambridge, UK: Woodhead Pub, 2010.

[2] H. Jiayi, J. Chuanwen, and X. Rong, "A review on distributed energy resources and MicroGrid", Renewable and Sustainable Energy Reviews, Elsevier, vol. 12, pp. 2472–2483, 2008

[3] J.M. Guerrero, "Connecting renewable energy sources into the smartgrid", 2011 IEEE International Symposium on Industrial Electronics (ISIE) , vol., no., pp.2400,2566, 27-30 June 2011.

[4] V.A. Boicea, "Energy Storage Technologies: The Past and the Present," Proceedings of the IEEE , vol.102, no.11, pp.1777,1794, Nov. 2014.

[5] M. Azubalis, A. Baranauskas, G. Tamulis, "Wind Power Balancing using Flywheel Energy Storage System", Elektronika ir Elektrotechnika, ISSN 1392-1215, Vol. 19, No. 1, 2013.

[6] J.M. Guerrero, M. Chandorkar, T.L. Lee, and P.C. Loh, "Advanced control architectures for intelligent microgrids—Part I: Decentralized and hierarchical control," IEEE Trans. Ind. Electron., vol. 60, no. 4, pp.1254–1262, Apr. 2013.

[7] J.M. Guerrero, J.C. Vásquez, J. Matas, L.G. deVicuña, and M. Castilla, "Hierarchical control of droop-controlled AC and DC microgrids—A general approach toward standardization," IEEE Trans. Ind. Electron., vol. 58, no. 1, pp. 158–172, Jan. 2011.

[8] G.M Toccaceli, P.E. Battaiotto, M.G. Cendoya, R.R. Peña, "RDG in weak grid for desalination plant. System topology and control strategy," Transmission and Distribution: Latin America Conference and Exposition (T&D-LA), 2012 Sixth IEEE/PES , pp.1,8, 3-5 Sept. 2012.

[9] M.G. Cendoya, G.M. Toccaceli, P.E. Battaiotto, "Wind generation applied to water desalination and H2 production in remote areas with weak networks", International Journal of Hydrogen Energy, Vol. 39, Issue 16, pp. 8827-8832, 2014.

[10] P.P. Parikh, M.G. Kanabar; T.S. Sidhu, "Opportunities and challenges of wireless communication technologies for smart grid applications," 2010 IEEE Power and Energy Society General Meeting, pp.1,7, 25-29 July 2010.